Geomorphic control of landscape carbon accumulation

Nan A. Rosenbloom,[1] Jennifer W. Harden,[2] Jason C. Neff,[3] and David S. Schimel[1]

Received 26 July 2005; revised 22 November 2005; accepted 7 December 2005; published 31 January 2006.

[1] We use the CREEP process-response model to simulate soil organic carbon accumulation in an undisturbed prairie site in Iowa. Our primary objectives are to identify spatial patterns of carbon accumulation, and explore the effect of erosion on basin-scale C accumulation. Our results point to two general findings. First, redistribution of soil carbon by erosion results in a net increase in basin-wide carbon storage relative to a noneroding environment. Landscape-average mean residence times are increased in an eroding landscape owing to the burial/preservation of otherwise labile C. Second, field observations taken along a slope transect may overlook significant intraslope variations in carbon accumulation. Spatial patterns of modeled deep C accumulation are complex. While surface carbon with its relatively short equilibration time is predictable from surface properties, deep carbon is strongly influenced by the landscape's geomorphic and climatic history, resulting in wide spatial variability. Convergence and divergence associated with upland swales and interfluves result in bimodal carbon distributions in upper and mid slopes; variability in carbon storage within modeled mid slopes was as high as simulated differences between erosional shoulders and depositional valley bottoms. The bimodality of mid-slope C variability in the model suggests that a three-dimensional sampling strategy is preferable over the traditional two-dimensional analog or "catena" approach.

Citation: Rosenbloom, N. A., J. W. Harden, J. C. Neff, and D. S. Schimel (2006), Geomorphic control of landscape carbon accumulation, *J. Geophys. Res.*, *111*, G01004, doi:10.1029/2005JG000077.

1. Introduction

[2] Soil is a major reservoir of carbon in terrestrial ecosystems. Most terrestrial landscapes are sloping and erosive but the current theory predicting large-scale patterns of soil organic carbon (C) accumulation is based on models where erosion and deposition are ignored or are assumed to be minimal [*Melillo et al.*, 1993]. While these C models represent climatic and particle size controls over soil carbon, they do not account for mobilization, erosional transport, deposition and fluvial transport [*Burke et al.*, 1989; *Schimel*, 1985; *Yonker et al.*, 1988]. Several continental-scale analyses have attempted to quantify the fate of eroded carbon [*Schlesinger*, 1995; *Smith et al.*, 2001]; however, these studies do not provide insight into the processes and mechanisms that operate at the landscape scale, regardless of whether storage or oxidation dominates. However, such local processes are known to affect storage and exchange of soil organic carbon [*Smith et al.*, 2001; *Stallard*, 1998; *Yoo et al.*, 2005], particularly in agricultural settings where erosion is greatly accelerated [*Harden*, 1999; *Liu et al.*, 2003; *Manies et al.*, 2001; *Schimel*, 1986; *Van Oost et al.*, 2003].

[3] There is a longstanding literature on sediment transport within catchments, yet few studies have tried to characterize the fate of advected carbon within upland basins, particularly in understanding how landscape and climate properties affect carbon mobilization and mean C age within a basin. Specifically, to what extent is mobilized carbon in sediments stored within a watershed, decomposed in situ, or exported to fluvial systems? For example, *Harden* [1999] and in tandem *Liu et al.* [2003] estimated that depending on the fate of its eroded carbon since the turn of the 19th century, an agricultural site in Mississippi could have been a large net source or a small net sink for C relative to a non-eroding history. This poorly constrained balance between the fate of in situ C and the potential export or burial of mobilized carbon is a limitation to estimating the terrestrial carbon budget [*Schlesinger*, 1995; *Smith et al.*, 2001; *Stallard*, 1998]. Specifically, we need to understand whether sedimentation acts as a mechanism for carbon sequestration [*Smith et al.*, 2001] and if so, for how long. Understanding the processes controlling the lateral transport of carbon is of special importance since erosion rates are changing worldwide with changing uses of the land. Natural disturbance and land-use change over the past century have altered natural disturbance regimes and accelerated erosion in many landscapes, evidence of which we see in near-surface sedimentary records [*Lal*, 1995; *Smith et al.*, 2001]. This recent change in disturbance regimes has not been fully evaluated in carbon cycle dynamics, yet potentially represents large fluxes of soil and carbon. Widespread depositional lowlands, which rep-

[1]National Center for Atmospheric Research, Boulder, Colorado, USA.
[2]U.S. Geological Survey, Menlo Park, California, USA.
[3]Benson Earth Sciences Building, University of Colorado at Boulder, Boulder, Colorado, USA.

0148-0227/06/2005JG000077$09.00

resent large C reservoirs, may release C upon land use disturbance or, alternatively, may store large amounts of C if these lands remain undisturbed.

[4] The fate of C within a small watershed is governed by interactive rates of sediment forcing and soil carbon turnover. However, most knowledge of soil carbon processing is based on studies of surface carbon dynamics in nonerosive settings. The interplay between sedimentation rate and carbon turnover is key to the potential for carbon storage in deep soils and sediment where it can be protected (i.e., sequestered) from decomposition or fire for long periods of time. In this paper we focus on (1) how climate and geomorphology interact to facilitate C storage/accumulation and (2) how erosion affects the mean age of C within a basin.

2. Methods

2.1. Site Description

[5] Our goal is to model a natural landscape in order to understand how erosion may explicitly affect C accumulation within an eroding basin. We base our model experiments on field observations of total soil carbon C and ^{10}Be collected along a hillslope catena [*Milne*, 1935] within the Dineson Prairie, in Western Iowa. The original data we use and all methods are reported by *Harden et al.* [2002] and *Manies et al.* [2001]. Replicate profiles were cored from three slope positions: stable ridge, eroding shoulder/transport slope, and depositional "lower" valley. The Dineson Praire preserve is 0.12 km^2 of grassland that was preserved as native tall grass prairie; responsibility for the site rests with the State Preserves Advisory Board, the Shelby County Preservation Board, and the Natural Resources Conservation Service. Since the late 1990s fire has been used every 2 years to reduce the influence of nonindigenous plants. Our samples were collected in 1997 (below) and therefore three to four recent fires have slightly reduced and transformed plant litter entering the surface soil. Fires were likely suppressed between about 1870 when farming practices commenced in the region until 1990. The small watershed has gentle, rolling (up to 12%) slopes with no perennial channels, gullies, or incised hollows evident, even after burning. Slopes range from 0 to 3% on ridgetops, 12% on the steepest midslope, and 0% on the depositional lowlands [*Harden et al.*, 2002]. This region of Iowa was ice-free during the last glacial advance [*Muhs and Bettis*, 2000]; soils are developed in loess (silt) deposits originating from glacial to post-glacial outwash along the Missouri River and distal loess sources in Nebraska [*Bettis*, 1990; *Muhs and Bettis*, 2000]. Soils are Mollisols (Monona series) with very deep, dark A horizons. Soils are predominantly silt (~70%) and clay (~29%) with very little sand (<2%). The upper soil layers are well mixed, with abundant evidence of widespread gopher activity.

2.2. Creep Model

[6] We use the Changing Relief and Evolving Ecosystems Program (CREEP) [*Rosenbloom et al.*, 2001] process-response model to simulate C and soil transport at the Dineson Prairie site. The CREEP model tracks the distribution of soil texture across a landscape through time by focusing on the differential movement of soil particles. Along with soil particles, CREEP also transports soil C (and other soil constituents) by two discrete mechanisms described below: diffusion of surface litter and advection of organic matter adhered to soil particles (primarily clay) in soil aggregates. CREEP simulates diffusive sediment transport according to a linear diffusion model, summarized by the equation

$$\frac{dz}{dt} = \left(\frac{\partial}{\partial x} k_x \frac{\partial z}{\partial x}\right) + \left(\frac{\partial}{\partial y} k_y \frac{\partial z}{\partial y}\right), \quad (1)$$

where x and y define orthogonal directions on a two-dimensional (2D) grid, z is the surface elevation, and k_x and k_y, indicate diffusivity in the x and y directions, respectively. Values of dz/dt less than zero indicate erosion; dz/dt greater than zero indicates deposition. This type of model responds to changes in the local curvature of the landscape. While all diffusion-based hillslope models simulate mass transport, the CREEP model is unique in that it was specifically developed to track the evolution of soil slope sequences by simulating the downslope fractionation of soil texture by particle size. Size fractionation and consequent spatial variation in soil texture are accomplished by allowing sand, silt and clay particles to move at different rates, controlled by the "effective" diffusivity, k_c, [*Koons*, 1989; *Rosenbloom et al.*, 2001] assigned to each particle size. While aggregation of clay particles to a larger size class in these fine-grained soils is likely, it is not specifically accounted for in the model. In this grassland environment, most of the downslope movement is diffuse rather than concentrated in rills or gullies and there was no field evidence for recent slope failure (e.g., landslides). Abundant gopher activity was evident from pervasive holes and filled burrows to depths of about 40 cm. Therefore soil transport by gophers and slope wash are both represented in the model as diffusive transport; while the relative importance of each agent is not known, the cumulative effect is assumed to be well represented by diffusion over model timescales. Overall landscape diffusivity ($\kappa_{clay} + \kappa_{silt} + \kappa_{sand}$), is constrained to ~1 m^2 ky^{-1} [*Martin and Church*, 1997; *Rosenbloom and Anderson*, 1994; *Rosenbloom et al.*, 2001]. We evaluate the "speed" (k_c) of one particle size relative to another by comparing the model output against observations. As the CREEP model modifies soil texture through time, it enables the preferential enrichment and burial of faster moving particles, which are typically fine-grained silts and clays.

[7] The CREEP model uses a decadal time step to simulate soil and landscape evolution across millennial timescales; these experiments encompass 4k model years, or 400 model time steps. Owing to the numerics, each time step is computationally expensive. Each pixel forms the surface layer for a vertical soil column; for these experiments we partition the soil columns into five soil layers with basal depths of 20, 50, 100, 150, and 200 cm. All transport takes place within the surface layer; there is no lateral communication between soil columns at depth. Erosion or deposition at the surface results in exhumation or burial of deeper soil layers. Accumulated carbon in the topsoil layer therefore can become buried and move downward in the soil column. Deep carbon may become exhumed at an

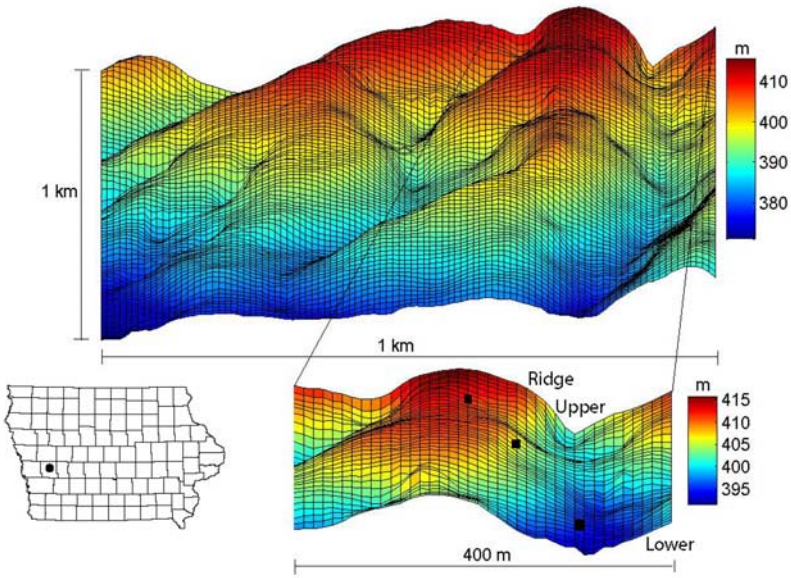

Figure 1. Dineson Prairie landscape in western Iowa. Digital Elevation Model (DEM) has 100 × 100 pixels with 10 m resolution. The Iowa map shows Shelby County, where the Dineson Prairie field observations were collected. The DEM inset shows a 40 × 40 cell subgrid basin used for model experiments with approximate locations of observations (Ridge, Upper, and Lower) and model grid cells used for experiments.

eroding site. Full domain experiments use a 100 × 100 cell 10 m resolution grid of the model domain. The experiments presented in this paper focus on a 40 × 40 grid subsection of the larger domain (Figure 1, insert). Comparisons between full-domain and subdomain results indicate that subdomain behavior scales linearly for this site. The domain choices are the result of balancing simulating significant landscape variability and ensemble size against computation.

2.3. Dust + 10Be

[8] We attempted to track dust deposition and sedimentation rates [*Brown*, 1987; *Harden et al.*, 2002; *McKean et al.*, 1993] using an isotopic tracer, ^{10}Be, which has a half-life ($t^{1/2}$ = 1.5 m.y.) much greater than our model timescales. ^{10}Be is produced in the atmosphere by collision of N and O [*Brown*, 1987; *Brown et al.*, 1981] and delivered to the system along with mineral dust (dry fall) and/or precipitation (wet fall) [*Monaghan et al.*, 1986]. Its relative insolubility, its atmospheric (surface) source, its strong sorption preference for clay particles, and its long half-life make ^{10}Be a powerful tracer for soil movement. In the CREEP model, mineral dust and wet fall ^{10}Be are both deposited as a uniform blanket across the landscape at each time step. We assign a dust delivery rate of 110 g/m^2/yr [*Harden et al.*, 2002], for 100 cm/yr rainfall, although past fluxes may have been up to 5 times greater than those of today [*Harden et al.*, 2002]. ^{10}Be delivery is assumed to have two components: dryfall (2.2×10^8 atoms/gDust) [*Harden et al.*, 2002], and wet fall (1.21×10^6 atoms/cm^2) [*Monaghan et al.*, 1986]. For modeling purposes we assume that ^{10}Be immediately adsorbs to clay particles and is advected along with clay as soil is redistributed through the landscape by erosion. By systematically adjusting dust flux (which also controls ^{10}Be delivery) and sediment transport parameters we attempted to constrain a best fit parameterization for dust and ^{10}Be delivery.

2.4. Carbon Flux

[9] Carbon inventories in all soil layers are governed by surface carbon content, which includes transport into or out of the surface layer. Subsurface carbon contents are linked to the surface via equation (6) (described below). CREEP partitions C into implied multiple soil pools (light and mineralized (heavy) fractions) by simulating two transport mechanisms: (1) diffusion of 20% of surface layer C as plant litter, and (2) passive advection of the remaining surface-layer C inventory as mineral-stabilized carbon (50% travels with clay, 35% with silt, and 15% with sand [*Schimel et al.*, 1994]). Movement of material into or out of the topsoil layer results in vertical advection of soil properties within a soil column, including soil texture, carbon, and ^{10}Be. In response to lateral and vertical fluxes of carbon into the surface layer, the model may accumulate or lose carbon within a soil column following the equations described below, moving the profile away from steady state,

$$\Delta C_{column} = \Delta C_{biological} + \Delta C_{transport}, \quad (2)$$

where the $\Delta C_{biological}$ is an implied in situ C uptake (photosynthesis minus respiration), parameterized in CREEP by equations (3) and (6); $\Delta C_{transport}$ is the net flux of advected and diffused carbon into and out of the cell.

2.5. Soil Carbon Dynamics

2.5.1. Surface Carbon

[10] Along with soil particles, CREEP simulates the downslope transport of surface soil C. CREEP uses a regression based on Century 4.0 [*Kelly et al.*, 1997] ecosystem model results, soil texture and local climate [*Kittel et*

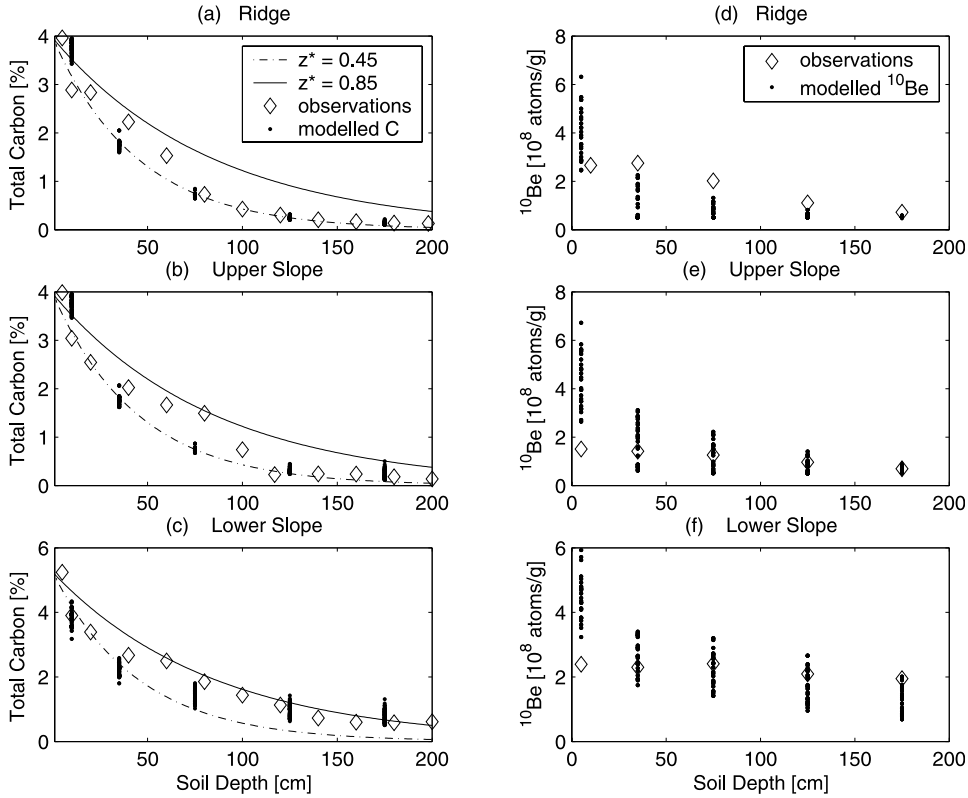

Figure 2. (a, b, c) Variations in observed deep C accumulation implying that C fluxes vary systematically between landscape positions and depend on slope morphology. Buried carbon in depositional areas is protected from decomposition, where turnover times appear to be attenuated relative to upper slope profiles. To simulate the adjustment in transient C storage in the model, we fit exponential decay curves to the data at each slope position. The solid and dashed lines in Figures 2a–2c indicate the theoretical z* curves for the two end-members used in all experiments. The black dots show the range of modeled C from the experiments highlighted in this paper. The difference between model and observed was used to estimate the cost function. Observed soil C falls off quickly with depth at the ridge sites (plot A) (z^* = 0.45 m) (equation (4)). However, observations at the lower slope diverge from the ridge-derived exponential (dashed line) (Figure 2c). Mid slopes are intermediate between the upper and lower slope values, possibly because they are alternately erosional/depositional through time. We note that discrepancies in modeled C accumulation in the top 20cm soil layer (Figure 2c) relative to observations are likely the result of incomplete assumptions as to C inputs as well as gradients in productivity or decomposition at this landscape position. (d, e, f) Observed ^{10}Be for the three landscape positions together with model-simulated ^{10}Be from all experiments. Note that CREEP consistently overestimates surface reserves of ^{10}Be, and underestimates ^{10}Be at depth on the ridge. Together, these plots illustrate the range of C and ^{10}Be values used in the cost function.

al., 1995] to estimate potential (equilibrium) soil C content [gC/m^2] for the topsoil layer,

$$C_{equil}(0) : 687 + 5462(\%\ \text{Clay}) + 2(\text{ET}) + 138(\text{MAT}) - 7(\text{MAT}^2), \quad (3)$$

where clay content in percent is averaged for the top 20 cm, ET is regional evapotranspiration [L/L^2], and MAT is mean annual temperature in degrees C. The model does not instantaneously achieve this potential carbon content but rather approaches it slowly as a function of the time constants described below (equations (5) and (6)). The model simulates gradients in productivity because surface C is a strong function of soil texture, which is allowed to change spatially [*Rosenbloom et al.*, 2001].

2.5.2. Deep Carbon

[11] CREEP does not simulate C fluxes at depth mechanistically. Rather, we impose a distribution of deep C that reflects observed C inventories and turnover times for specific landscape positions. As carbon moves to or from a particular landscape position, decomposition/preservation of advected carbon is simulated on the basis of its landscape position (e.g., carbon, regardless of origin, decomposes differently on a hilltop versus a swale). We assume that ridge profiles reflect C turnover in the absence of significant erosion or burial. Plotting the observed C depth profiles for the ridge site we fit an exponential decay curve to the data (z^*; Figure 2),

$$C_{equil\,(z)} = C_{equil\,(0)}\left[e^{(-z/z^*)}\right], \quad (4)$$

where C is total soil carbon [gC/m^2], $C_{equil(0)}$ is the idealized carbon content of the surface layer based on climate and soil texture (from equation (3)), $C_{equil(z)}$ is the expected C at depth z, and z^* is an empirical depth scaling. The actual C content in any layer will often differ from the potential C content because of C transport into and out of the surface layer. On the basis of the ridge profile we estimate a z^* value of 0.45 m (Figure 2a), which can be interpreted as the C depth attenuation where C at 1 m will be roughly 10% of the surface value, a trend that is comparable to the depth attenuation of soil radiocarbon data at these [*Harden et al.*, 2002] and other sites [*Trumbore et al.*, 1995]. However, soil profiles taken from the lower slopes have more carbon in the deep soil, and were best fit by a z^* value of between 0.65 and 0.85 m (Figure 2c), implying that C at 1 m will retain as much as 30% of the surface inventory. Increased C at depth in the lower slopes suggests a longer turnover time, which is in agreement with radiocarbon data collected on site [*Harden et al.*, 2002]. While we do not simulate the increased carbon storage mechanistically, we force the model to reproduce the observations by spatially varying the z^* scale factor. Eroding, upland cells are assigned a z^* of 0.45. Depositional lowland cells, are assigned a z^* of 0.85, consistent with observations.

[12] The model accounts for disequilibria between the theoretical steady state ($C_{equil(0)}$) and the actual C inventory at time t ($C_{actual(0)}$)as a function of the adjustment timescale (ATS), which increases exponentially with depth in the soil column. The ATS can be thought of as a relaxation time, analogous to a mean residence time, or the time required for the model to return to equilibrium after a change of state (e.g., erosion or deposition),

$$ATS_{(z)} = ATS_{(0)}\left[e^{(2.6z)}\right], \quad (5)$$

where $ATS_{(0)}$ is the mean residence time at the surface (30 years [*Manies et al.*, 2001], although a range of values is considered for our modeling scenarios) and $ATS_{(z)}$ is the mean residence time at depth; roughly 400 years at 1 m, based on the ridge profile. Carbon inventories in all soil layers are updated at each time step to account for decomposition or accumulation,

$$C^{t+1}_{actual\,(z)} = C_{equil(z)} - \left[C_{equil\,(z)} - C^{t}_{actual\,(z)}\right] * \left[e^{(-dt/ATS(z))}\right], \quad (6)$$

where $C_{equil(z)}$ [gC/m^2] is the storage potential of layer z (equation (4)), $C^t_{actual(z)}$ [gC/m^2] is the C inventory at time t, and $C^{t+1}_{actual(z)}$ is the C storage at time $t + 1$. Note that C_{actual} reflects both C production and implied decomposition.

2.6. Model Initialization

[13] We run CREEP as a forward model, classifying the evolving landscape as an "open" system which contains no unique or finite solution. As such, the model output is strongly dependent on the choice of initial conditions including soil texture and landscape form, and on time-dependent forcing such as climate, all of which are unknowable but can be generally inferred from the present landscape. Given this landscape, we make several primary assumptions about the Dineson Prairie: (1) that the site has remained without major morphological change for at least the past 10 ky, (2) that the landscape is gradually being reduced by diffusive processes (section 2.2) through time, (3) that dust fluxes were likely to have been much greater in the past [*Harden et al.*, 2002] and dust continues to be a significant soil input, and (4) that the dominant vegetation has been prairie grassland for the past 8 ky [*Collins and Wallace*, 1990].

[14] We use a 100 × 100 cell USGS Digital Elevation Model (DEM) at 10-m resolution as our base topography. However, we initialize each model run by numerically stretching the original DEM terrain to create a more "youthful" topography, artificially sharpening prominent landscape features and increasing the topographic relief between valleys and ridge tops. As the model runs forward in time the "youthful" terrain relaxes toward the actual landscape. Moderately rejuvenating the terrain allows us to retain realistic slope gradients throughout the experiment (during which time diffusion is operating continuously to reduce the slope). We drape a soil of uniform thickness and composition across the model domain using basal layer soil texture from the ridge soil core (69% silt, 29% clay). We assume that ridge data ideally reflect an unbiased sample of parent material. Dust is deposited at each time step as a uniform blanket across the landscape at a time-dependent rate (section 2.3). Given that the observed soil is primarily loess, we assign the composition of deposited dust to be roughly that of the underlying material (25% clay, 75% silt).

2.7. Model Evaluation

[15] To parameterize the model for Dineson Prairie we found the most likely scenario for particle transport efficiency (κ_{sand}, κ_{silt}, κ_{clay}) and dust delivery by varying characteristics of the model and running it for 4000 years and comparing the results to observations. We run the model for 4000 years because the topography of the evolving "rejuvenated" landscape is most similar to the actual landscape after 3500–4500 model years. We then created four primary estimates of long-term mean conditions using a range of parameters related to turnover because these parameters are not well constrained by observations. The base simulation (Figure 3) is thus an average of four model runs wherein we alternated surface C residence time ($ATS_{(0)}$, equation (5)) between 30 and 78 years, and the depth scaling for turnover (z^*, equation (4)) between 0.65 and 0.85 m for lower slopes.

[16] To test C storage sensitivity to environmental forcing, we examined the model response to episodic excursions from the four primary estimates of long-term mean conditions using a set of three "forcing" scenarios. In the first scenario only sediment transport rates were allowed to vary (Erosion Only). In the second scenario, only dust and ^{10}Be (wet fall) rates were allowed to change (Dust Only). In the third scenario, both sediment transport and dust delivery were altered (Dust + Erosion) (Figure 3). Each forcing scenario contains 10 ensemble members in which we perturbed the best fit model estimates for long-term mean dust flux and transport efficiency at arbitrary intervals within a 4000-year model run in order to track overall model response to disturbance. Within these ensemble runs, transport efficiencies (diffusivity) and dust delivery rates

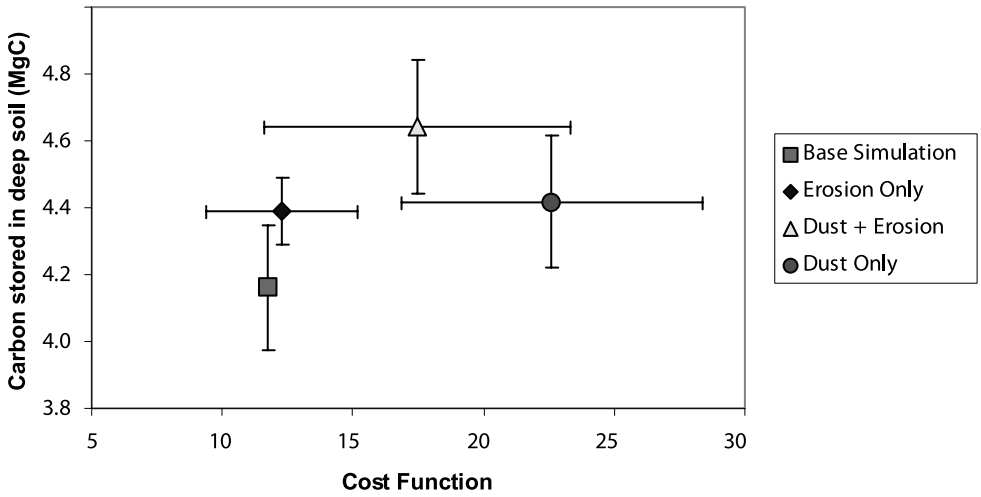

Figure 3. Sensitivity of C storage to model forcing, with comparison of the base simulation (dust and erosion constant) to three scenarios: Erosion Only (dust constant), Dust Only (erosion constant), and Dust + Erosion (variable dust and erosion). Each scenario represents an ensemble of 10 perturbations of 4 primary cases for a total of 40 individual runs. The base simulation is an average of four estimates for C storage (see text). The value reported for each ensemble member is the landscape-average C content. The x axis shows the average cost function (CF) for each scenario; the y axis demonstrates the effect of forcing on deep C storage. To estimate the CF for each experiment we compared modeled soil texture (% clay), C and ^{10}Be against observations from five soil depths (10, 35, 75, 125, and 175 cm) at three landscape positions (ridge, upper slope, and valley). Successful (low CF) modeling runs consistently reflect modest changes in dust flux, with or without concurrent changes in erosion. Larger changes in dust flux resulted in higher CFs, and were therefore more likely to be rejected as implausible. Note that highly unrealistic model runs (CF > 50) were not included as ensemble members.

were altered within an order of magnitude. The duration of model perturbations varied from 100 to 2000 years, with up to seven interludes within the 4 ky run. We repeated these experiments for each of the four primary cases for a total of 40 individual runs per scenario. The four primary cases capture a range of uncertainty in C parameterization, while the three forcing scenarios offer a range of uncertainty in the geomorphic processes.

[17] As a metric for model resemblance to the observations we developed a multivariate "cost function," or "goodness-of-fit" estimate which provides a quantitative measure of how well the model reproduces the observations through time. The cost function is estimated as the sum of squares between model and observations at three landscape positions (ridge, upper slope, and valley) for ^{10}Be, carbon, and soil texture (% silt and clay). All sites include soil profile observations, which we compare against five CREEP layer estimates to 2 m. We estimated the cost function by comparing the model against observations at the end of 4000 model years. Successful model runs are able to reproduce soil textural variation, ^{10}Be distributions, and soil C accumulations. The cost function allowed us to reject some forcing scenarios as implausible, while retaining others. Thus, while we cannot propose a single most plausible forcing scenario, we can reject a significant number of possibilities as discussed below.

3. Results and Discussion

[18] We use the CREEP model to explore the effects of erosion on landscape carbon accumulation. We focus on an ensemble of forcing scenarios that test the sensitivity of our results to initial conditions and environmental forcing. The forcing scenarios that are most plausible have in common several characteristics including (1) modest changes in dust flux, particularly toward the present, (2) modest episodic changes in sediment transport, or (3) concurrent episodic changes in both dust flux and erosion. Sustained or extreme excursions away from base conditions by either dust flux or erosion produced unreasonably high cost functions, and therefore, unrealistic results. Overall, redistribution of soil carbon by erosion resulted in a net increase in mean carbon storage irrespective of forcing mechanism (Figure 3). Shifts in dust delivery accompanied by changes in sediment transport rates produced the highest increases in total C storage. Episodic variations in parameter forcing, particularly dust delivery, increased deep carbon storage relative to experiments driven by uniform forcing. Our results consistently indicate that estimates of mean landscape C storage may be as much as 40% too low when transport and redeposition of C are ignored. This result is robust even when we impose a spatially uniform parameterization of C storage (z^*) (section 2.5.2, Figure 2a, and Figure 4, Uniform Turnover). The spatial variation in carbon represents a combination not only of interactive processes such as erosion/deposition, dust, depth attenuation of C turnover (z^*), and net primary production but also of historic changes in these processes. Fundamentally, the modeled increase in landscape C with advection is a consequence of the differential sorting, enrichment and stabilization of C, because turning off differential C movement results in zero increase in overall landscape C over a level landscape (results not

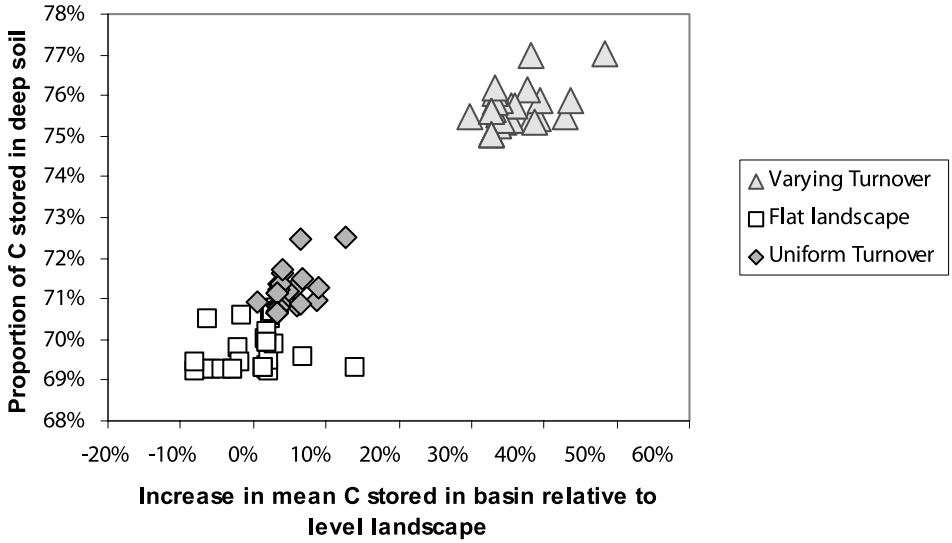

Figure 4. Sensitivity of C storage to turnover and erosion. Three experiments illustrate the effect of spatially varying the depth-dependency of C turnover on C accumulation. The diamond and triangle symbols represent spatially uniform and spatially varying turnover (z*). The square symbol represents the value for a landscape with no lateral transport but with varying dust deposition. Each point with a common symbol represents a model run with distinct forcing (e.g., Dust Only, Erosion Only), averaged over four model runs with different C parameter values (section 2.7). Forcing for individual runs was identical for each set of symbols; only turnover (z*) is treated differently for each symbol. Allowing turnover to vary spatially in an eroding landscape clearly has the greatest effect on C storage. However, spatially uniform turnover in an eroding landscape results in greater overall C accumulation relative to a level landscape.

shown). *Harden et al.* [2002] sampled ^{10}Be at this site and we simulated and used in our cost function (Figure 3) the import and transport of ^{10}Be. However, in a landscape of this complexity, information from the ^{10}Be as sampled along one slope sequence, or 2D catena, placed only a weak constraint on ^{10}Be accumulation, and implicitly, on dust deposition and sedimentation. We believe there may be several explanations for this: (1) multiple model input paths, and possible multiple transport paths, (2) unrepresentative field samples relative to landscape complexity, and (3) hillslope convergence/divergence that has affected the redistribution of clay (and hence ^{10}Be) in the model in ways we do not understand.

3.1. Simplification of Carbon Cycle

[19] Continental-scale redistribution of carbon due to erosion has received significant attention [*Schlesinger*, 1995; *Smith et al.*, 2001]. At the scale of hillslopes, however, carbon can be moved horizontally and vertically in soils and this process represents a nonsteady state transfer of carbon from short to long residence time soil organic matter pools. In the same way that aggregate formation [*Six et al.*, 2000] and soil mineral stabilization of carbon [*Kaiser and Zech*, 1998] can increase the mean residence time of carbon in a landscape, so too can erosional burial of carbon on eroding hillslope sequences. Understanding how turnover (inputs and decomposition) varies as a function of depth, burial, and erosion is of central importance to C storage estimates in dynamic landscapes. While we do not address the mechanisms that can act to slow decomposition in buried sediments directly in this analysis, it is clear that this slowing effect is important, at least in fine-grained soils [*Wynn et al.*, 2005]. Microbial protection and stabilization, stabilization by organo-mineral complexes [*Torn et al.*, 1997], and slowing of turnover by substrate limitation are but a few mechanisms that might contribute to the reduction of decomposition at depth. However, each mechanism could respond quite differently to erosion, transport and deposition and thus future models should incorporate advances in these fields.

3.2. Spatial Variability in Carbon Age: The Deep Carbon Conundrum

[20] Deep carbon in lowland areas appears to be protected from decomposition in a way unlike that of the ridge and mid slope. In this regard, the model simply reproduces landscape averaged turnover times but can also be used to examine the importance of deposition-decomposition interactions. The simulations illustrate the large impact that slower lowland C turnover can have on landscape carbon stabilization and suggest the need for better mechanistic understanding of controls on carbon turnover across geomorphically complex landscapes. The variations in deep C accumulation imply that decomposition dynamics vary systematically between landscape positions and depend on slope morphology. Explanations for systematic variations in decomposition are complex because we do not know whether turnover is attenuated by depth or by age of the C substrate [*Harden et al.*, 2002] or may reflect the residual signature of historically higher NPP in valley bottoms. Regardless of the mechanism for greater C storage in deep soil layers, the net effect of C burial results in a significant sequestration for at least as long as C remains buried.

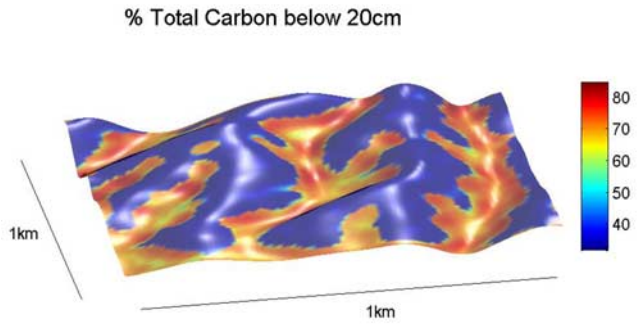

Figure 5. Percent total carbon stored in deep soil layers (>20 cm). This figure illustrates that C accumulation is not spatially uniform. High concentrations of C are found at the lower mid slopes where the slope gradient and subsequent transport have been reduced, favoring burial and accumulation of soil carbon. Peak carbon accumulation reflects the redistribution of C along converging flowpaths. Total landscape relief is 45 m.

3.3. Influence of Geomorphology on Carbon Storage

[21] Subtle slope dynamics produced three-dimensional patterns of C storage that were far more complex than a first-order C inventory based on elevation or slope position alone. While surface carbon with its relatively short equilibration time was predictable from dominant soil properties such as climatic parameters and clay content, deep carbon was strongly influenced by geomorphology. Figure 5 shows that C accumulation is not spatially uniform and that C storage peaks at the base of convergent swales. High concentrations of C are found in the surface layers of the lower mid slopes where the slope gradient and subsequent transport have been reduced and C is allowed to concentrate. In lowland soils, deep layers store the majority of soil carbon, particularly along drainage axes.

[22] Subtle terrain features, particularly convergent flowpaths where sediment can be focused, have a particularly strong effect on the heterogeneity of soil carbon storage. Carbon distribution on mid-slopes was particularly heterogeneous and varied significantly in response to comparatively subtle changes in terrain features. C accumulation is strongly and pervasively bimodal across much of the mid slopes (Figure 6). Undulations, or microtopography, made of low-carbon interfluves and high-carbon flow paths, change over the course of the slope development and, as a result, produce bimodal distributions of carbon. Over time, these microtopographic features change, as do the distributions of carbon, rendering the mid slope a particularly heterogeneous component of the landscape. Upland slopes have relatively less C accumulation (Figures 6a and 6b), but some cells do accumulate C even near the ridge (Figure 6b). Lowland cells, in contrast, store more C overall (Figure 6e).

3.4. Implications for Sampling Soils

[23] On the basis of the pattern of complexity shown in Figures 5 and 6, the conceptual model of landscape carbon distribution that has implicitly guided most ''catena'' sampling schemes may miss important intraslope variability. Most studies of landscape carbon accumulation assume that the structure of variability within a slope can be explained using a 2D analog and focus on samples taken from ridgetop, slope and valley components. The amount of replication within these components varies but normal variability within slope classes is assumed to be random error and no analyses have also considered structure within slope classes. In reality, the 3D evolution of landscapes and soils dictates that a single depth profile may reflect some combination of historical convergent or divergent flow. CREEP results show that this 3D structure exerts a strong influence over carbon accumulation, especially when carbon below the surface layer is included in the analysis. An improved sampling strategy would replicate sampling of the mid slopes as well as identify a small number of new slope categories (convergent and divergent flow sites that exist today on slopes and in drainages), potentially improving our ability to extrapolate from point measurements to landscape averages. The CREEP model can be used to refine sampling strategies, and to improve attempts to scale from landscape characteristics to landscape carbon content.

3.5. Erosion-Production Interactions

[24] Interactions between NPP and soil fertility during erosion/burial, for example, erosion-production interactions, could easily enhance the C sequestration effect if soil fertility were maintained (in, for example, fertilized hillslopes or areas with high dust flux) or could offset the C sequestration effect if soil fertility were reduced by erosion. Alternatively, *Porder et al.* [2005] have demonstrated that erosion can enhance the availability of mineral-derived nutrients, illustrating that erosion-production interactions are complex. The balance between erosion and plant production has been used to interpret sustainability and erosion tolerance [*Sparovek and Schnug*, 2001], yet if we are also to consider greenhouse gases for resource management, then a full accounting must also include input rates by dust and fertilizer, storage by deep burial, and as is borne out by our study, the dynamic nature of C transport, burial, and exposure. At large spatial scales, erosional carbon sinks require new productivity to replace eroded material [*Stallard*, 1998]. This can be accomplished in agricultural settings through fertilization, which allows net primary production to be maintained despite erosional loss of soil nutrients [*Stallard*, 1998]. In natural (nonagricultural) environments, weathering and dust contributions can maintain inputs of rock-derived nutrients; however, N fixation and/or deposition would have to keep pace with erosion and dust inputs for overall landscape NPP is to be maintained.

4. Conclusions

[25] The CREEP experiments strongly suggest two important conclusions. The first is that field sampling strategies that rely on traditional slope designations may overlook important variations of C storage within a slope. This result arises from convergent/divergent flow patterns which not only concentrate flow, but change through time such that pockets of accumulation high on a slope may hold as much C in deep soil layers as areas much lower on the slope. The second conclusion is that regional estimates of soil carbon extrapolated from 1D vertical profiles could greatly underestimate the total C in a landscape with even moderate topographic relief. Primarily this is because of the enhanced

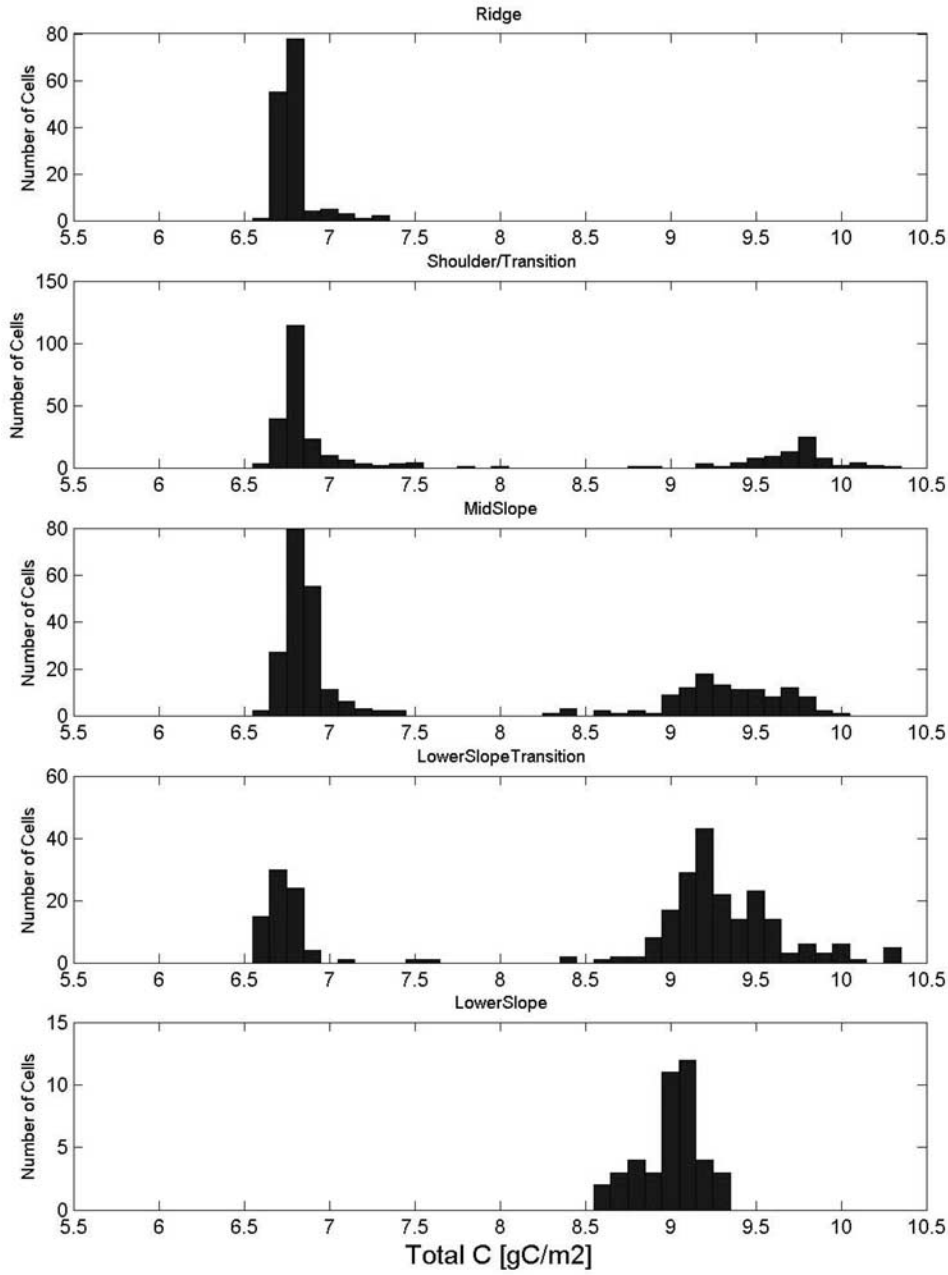

Figure 6. Carbon distributions across landscape positions. Convergent/divergent flowpaths in a three-dimensional landscape strongly affect total C storage within generalized landscape positions. Model results are shown for one 4 ky model run; distribution details vary by forcing scenario but the general pattern of bimodel C distribution is repeated for each of 120 model runs. Each histogram shows C accumulation at different hillslope positions, represented by a landscape-wide assessment of pixels along contours of constant elevation. The top contour panel represents the stable ridge; the bottom panel represents the base of the slope, where deposition has been continuous. The transitional shoulder and midslope positions have strongly bimodal C accumulation, illustrating the effect of local convergence/divergence patterns on net C accumulation within similar geomorphic positions.

C storage resulting from sediment/carbon mobilization and burial. Other origins for C retention in depositional slopes have been demonstrated to be important (e.g., enhanced plant inputs [*Yoo et al.*, 2005]), but the net enhancement of C storage in depositional settings is universally underestimated by model parameterizations of ''flat'' landscapes. Carbon content of a typical level upland site (Figure 4, Flat Landscape), for example, is representative of most large-scale models [*Burke et al.*, 1989], which build upon regional estimates by assuming that a non-eroding site is representative of regional carbon storage. Every 1D C model that ignores erosion implicitly assumes that landscape redistribution of C has no net effect on C storage, or that carbon movement across a landscape results in a landscape average

that is no different from the 1D estimate. Our results suggest that scaling from these traditional estimates of carbon content results in a substantial underestimate of C stores for real landscapes with potential for lateral redistribution. Redistribution that leads to burial of C appears to increase landscape-average carbon age owing to the preservation of otherwise labile C. Conversely, direct export of C from a rapidly eroding watershed would result in a decrease in landscape-average carbon age. The CREEP model suggests that locally redeposited sediment adds a directional bias to net C storage by increasing mean C age at the catchment scale. Depending on the intensity of deposition, the complexity of the local erosional history, and the assumptions made for mean residence times, the contribution of landscape processes could be as much as 40% of carbon inventories. We hypothesize that the landscape-average age of soil carbon in a topographically complex environment will always exceed the age of C in a level environment given equivalent NPP.

[26] **Acknowledgments.** Primary funding for this work came from USGS-02WRAG0048. The National Center for Atmospheric Research is sponsored by the National Science Foundation. We thank Tom Hilinksi and Becky McKeown for their help in rewriting the CREEP code from C to C++, and David Baker (NCAR) for many helpful discussions on model optimization. We also thank our reviewers for their many thoughtful comments on this manuscript.

References

Bettis, E. A. I. (1990), The Deforest formation of western Iowa: Lithologic properties, stratigraphy and chronology, report, 96 pp., Soil Conserv. Serv., U.S. Dep. of Agric., Washington, D. C.

Brown, L. (1987), 10Be: Recent applications in Earth sciences, *Philos. Trans. R. Soc. London*, *323*, 75–88.

Brown, L., I. S. Sacks, F. Tera, and R. Middleton (1981), Beryllium-10 in continental sediments, *Earth Planet. Sci. Lett.*, *55*, 370–376.

Burke, I. C., C. M. Yonker, W. J. Parton, C. V. Cole, K. Flach, and D. S. Schimel (1989), Texture, climate, and cultivation effects on soil organic-matter content in US grassland soils, *Soil Sci. Soc. Am. J.*, *53*, 800–805.

Collins, S. L., and L. L. Wallace (1990), *Fire in North American Tallgrass Prairies*, 175 pp., Univ. of Okla. Press, Norman.

Harden, J. W. (1999), Dynamic replacement and loss of soil carbon on eroding cropland, *Global Biogeochem. Cycles*, *13*(4), 885–901.

Harden, J. W., T. L. Fries, and M. J. Pavich (2002), Cycling of beryllium and carbon through hillslope soils in Iowa, *Biogeochemistry*, *60*, 317–336.

Kaiser, K., and W. Zech (1998), Soil dissolved organic matter sorption as influenced by organic and sesquioxide coating and sorbed sulfate, *Soil Sci. Soc. Am. J.*, *62*, 129–136.

Kelly, R. H., W. J. Parton, G. J. Crocker, P. R. Grace, J. Klir, M. Korschens, P. R. Poulton, and D. D. Richter (1997), Simulating trends in soil organic carbon in long-term experiments using the century model., *Geoderma*, *81*, 75–90.

Kittel, T. G. F., N. A. Rosenbloom, T. H. Painter, and D. S. Schimel (1995), The VEMAP integrated database for modeling United States ecosystem/vegetation sensitivity to climate change, *J. Biogeogr.*, *22*, 857–862.

Koons, P. O. (1989), The topographic evolution of collisional mountain belts: A numerical look at the Southern Alps, New Zealand, *Am. J. Sci.*, *289*, 1041–1069.

Lal, R. (1995), Global soil erosion by water and carbon dynamics, in *Soil Global Change*, edited by R. Lal et al., pp. 131–142, CRC Press, Boca Raton, Fla.

Liu, S. G., N. Bliss, E. Sundquist, and T. G. Huntington (2003), Modeling carbon dynamics in vegetation and soil under the impact of soil erosion and deposition, *Global Biogeochem. Cycles*, *17*(2), 1074, doi:10.1029/2002GB002010.

Manies, K. L., J. W. Harden, L. Kramer, and W. J. Parton (2001), Carbon dynamics within agricultural and native sites in the loess region of western Iowa, *Global Change Biol.*, *7*(5), 545–555.

Martin, Y., and M. Church (1997), Diffusion in landscape development models: On the nature of basic transport relations, *Earth Surf. Processes Landforms*, *22*, 273–279.

McKean, J. A., W. E. Dietrich, R. C. Finkel, J. R. Southon, and M. W. Caffee (1993), Quantification of soil production and downslope creep rates from cosmogenic Be-10 accumulations on a hillslope profile, *Geology*, *21*(4), 343–346.

Melillo, J. M., A. D. McGuire, D. W. Kicklighter, B. Moore, C. J. Vorosmarty, and A. L. Schloss (1993), Global climate-change and terrestrial net primary production, *Nature*, *363*(6426), 234–240.

Milne, G. (1935), Some suggested units of classification and mapping particularly for East African soils, *Soil Res.*, *4*, 3.

Monaghan, M. C., S. Krishnaswami, and K. K. Turekian (1986), The global average production rate of 10Be, *Earth Planet. Sci. Lett.*, *76*, 51–60.

Muhs, D. R., and E. A. I. Bettis (2000), Geochemical variations in Peoria loess of western Iowa indicate paleowinds of midcontinental North America during last glaciation, *Quat. Res.*, *53*, 49–61.

Porder, S., A. Paytan, and P. M. Vitousek (2005), Erosion and landscape development affect plant nutrient status in the Hawaiian Islands, *Oecologia*, *142*(3), 440–449.

Rosenbloom, N. A., and R. S. Anderson (1994), Hillslope and channel evolution in a marine terraced landscape, Santa Cruz, California, *J. Geophys. Res.*, *99*, 14,013–14,029.

Rosenbloom, N. A., S. C. Doney, and D. S. Schimel (2001), Geomorphic evolution of soil texture and organic matter in eroding landscapes, *Global Biogeochem. Cycles*, *15*(2), 365–381.

Schimel, D. S. (1985), Soil organic matter dynamics in a paired rangeland and cropland toposequences in North Dakota, *Geoderma*, *36*, 201–214.

Schimel, D. S. (1986), Carbon and nitrogen turnover in adjacent grassland and cropland ecosystems, *Biogeochemistry*, *2*, 345–357.

Schimel, D. S., B. H. Braswell, E. A. Holland, R. McKeown, D. S. Ojima, T. H. Painter, W. J. Parton, and A. R. Townsend (1994), Climatic, edaphic and biotic controls over storage and turnover of carbon in soils, *Global Biogeochem. Cycles*, *8*(3), 279–293.

Schlesinger, W. H. (1995), Soil respiration and changes in soil carbon stocks, in *Biotic Feedback in the Global Climatic System: Will the Warming Feed the Warming*?, edited by G. M. Woodwell and F. T. Mackenzie, pp. 159–168, Oxford Univ. Press, New York.

Six, J., K. Paustian, E. T. Elliott, and C. Combrink (2000), Soil structure and soil organic matter: I. Distribution of aggregate size classes and aggregate associated carbon, *Soil Sci. Soc. Am. J.*, *64*, 681–689.

Smith, S. V., W. H. Renwick, R. W. Buddemeier, and C. J. Crossland (2001), Budgets of soil erosion and deposition for sediments and sedimentary organic carbon across the conterminous United States, *Global Biogeochem. Cycles*, *15*(3), 697–707.

Sparovek, G., and E. Schnug (2001), Temporal erosion-induced soil degradation and yield loss, *Soil Sci. Soc. Am. J.*, *65*, 1479–1486.

Stallard, R. F. (1998), Terrestrial sedimentation and the carbon cycle: Coupling weathering and erosion to carbon burial, *Global Biogeochem. Cycles*, *12*(2), 231–257.

Torn, M. S., S. E. Trumbore, O. A. Chadwick, P. M. Vitousek, and D. M. Hendricks (1997), Mineral control of soil organic carbon storage and turnover, *Nature*, *389*(6647), 170–173.

Trumbore, S. E., E. A. Davidson, P. Barbosa de Camargo, D. C. Nepstad, and L. A. Martinelli (1995), Belowground cycling of carbon in forests and pastures of Eastern Amazonia, *Global Biogeochem. Cycles*, *9*(4), 515–528.

Van Oost, K., W. Van Muysen, G. Govers, G. Heckrath, T. A. Quine, and J. Poesen (2003), Simulation of the redistribution of soil by tillage on complex topographies, *Eur. J. Soil Sci.*, *54*, 63–76.

Wynn, J. G., M. I. Bird, and V. N. L. Wong (2005), Rayleigh distillation and the depth profile of $^{13}C/^{12}C$ ratios of soil organic carbon from soils of disparate texture in Iron Range National Park, Far North Queensland, Australia, *Geochim. Cosmochim. Acta*, *69*(8), 1961–1973.

Yonker, C. M., D. S. Schimel, E. Paroussis, and R. D. Heil (1988), Patterns of organic carbon accumulation in a semiarid shortgrass steppe, Colorado, *Soil Sci. Soc. Am. J.*, *52*, 478–483.

Yoo, K., R. Amundson, A. M. Heimsath, and W. E. Dietrich (2005), Erosion of upland hillslope soil organic carbon: Coupling field measurements with a sediment transport model, *Global Biogeochem. Cycles*, *19*(3), GB3003, doi:10.1029/2004GB002271.

J. W. Harden, U.S. Geological Survey, 345 Middlefield Road, Menlo Park, CA 94025, USA.

J. C. Neff, Benson Earth Sciences Building, Campus Box 399, 2200 Colorado Avenue, University of Colorado at Boulder, Boulder, CO 80309, USA.

N. A. Rosenbloom and D. S. Schimel, National Center for Atmospheric Research, 1850 Table Mesa Drive, Boulder, CO 80305, USA. (nanr@ucar.edu)